PCCP

Accepted Manuscript

ROYAL SOCIETY OF CHEMISTRY

www.rsc.org/pccp

A Combined Molecular Dynamic and Quantum Mechanic Study of the Solvent and Guest Molecule Effect on the Stability and Length of Heterocyclic Peptide Nanotube

Mohammad Izadyar*, Mohammad Khavani, Mohammad Reza Housaindokht

Department of Chemistry, Faculty of Sciences, Ferdowsi University of Mashhad, Mashhad, Iran

izadyar@um.ac.ir

Telefax: +985138795457

Abstract

Molecular dynamic simulations have been performed for investigation of the stability of heterocyclic peptide nanotube composed of 1,4-disubstituted-1,2,3-triazol ε-amino acid. 45 ns MD simulations on the cyclic peptide nanotube (CPNT) and cyclic peptide dimer in methanol, chloroform and water reveal that these structures are more stable in the nonpolar solvents. MM-PBSA and MM-GBSA calculations have been employed to analyze the solvent effect on the stability and length of CPNT. These calculations showed that CPNT in chloroform was more stable and longer that other solvents. Effect of Guest molecule (ethanol) inside the dimer and CPNT was investigated, too. Obtained results confirmed that guest molecule(s) stabilized the dimer and CPNT in all solvents. Quantum chemistry

calculations on the cyclic peptide dimer have been performed at the M06-2X/6-31G(d) level in the gas phase and three solvents. Obtained results from quantum chemistry study were in good agreement with the MD simulation results. DFT calculations showed that guest molecule stabilized the dimer structure and has electrostatic interaction with cyclic peptide dimer. Finally, for investigation of the solvent effects on the hydrogen bonds of cyclic peptide dimer NBO and AIM analysis have been performed.

Keywords: Peptide nanotube; Molecular dynamics; Quantum mechanics; Stability; Hydrogen bond; Electron localization function

Introduction

Cyclic peptides (CPs) have been considered in recent years as a remarkably versatile approach to the formation of organic nanotubes. These cyclic peptides consist of 6–10 alternating D- and L-α-amino acid residues,[1] cyclic β-peptides [2,3] and cyclic peptides containing alternating α- and γ- or α- and ε-residues [4–6]. Nanotechnology concerns the preparation and characterization of the structures on the nanometer scale and the use of such systems as novel functional materials and devices.[7]

Nanotubes are particularly interesting structures because of their many applications in different fields such as molecular separation and transport,

catalysis, optics, electronics, chemotherapy and drug delivery.[8] For example Subramanian and co-workers investigated the ability of some CPNTs for transportation of the antitumor drug (5-fluorouracil) across the lipid bilayer, theoretically.[9] solvents and amino acid composition are important parameters involved in the stability of CPNT structures. Previous theoretical studies indicate that these structures are more stable in nonpolar solvents.[10,11] Some materials such as zeolites, graphite, inorganic complexes, lipids and cyclodextrins can make nano tubular structures.[12] Covalently bonded nanostructures have been thoroughly studied in past few decades but today, non-covalently bonded nanotubes are in attention because of their many applications in different fields. [13]

There are many different routes by which hydrogen bonds can be used to self-assemble nanotubes. Gramicidin A is perhaps the first and well-known structure of the coiling of the linear peptides which has a tubular structure and known as β-helices, [14,15] although there are many others that have since been discovered including forty eight residue polytheonamides.[16,17] Another example is the assembly of lanreotide peptides into nanotubes assembly, producing tubes which has larger internal diameters.[18]

Nanotubes can also be assembled from sector-like molecules, as in the case of the tobacco mosaic virus (TMV), which consists of a tubular structure of unimeric coat proteins that undergoes self-assembly around a single strand of

RNA.[19] But the cyclic peptide nanotubes have better efficiency than gramicidin A or other structures for transporting molecules and ions. The ion transport rates of the self-assembled peptide channels are greater than those of the very efficient and widely-studied gramicidin A channel.[20]

In this paper we investigate the stability of a heterocyclic peptide nanotube and its dimer consist of 1,4-disubstituted-1,2,3-triazol ε-amino acid (Scheme 1), in methanol, water and chloroform. Additionally, the effect of ethanol as a guest molecule on the stability of cyclic peptide nanotube (CPNT) and its dimer was investigated. Tubular ensemble made up of eight cyclic peptides (CPs) was chosen for this study as cyclic peptide nanotube because of long length (42 Å). Here, we present the results of 45 ns molecular dynamic simulation (MD) on the dimer and CPNT in water, methanol and chloroform. Finally quantum mechanics studies such as, DFT calculations, natural bond orbital analysis and quantum theory of atom in molecule (QTAIM) on the dimer of cyclic peptide have been performed.

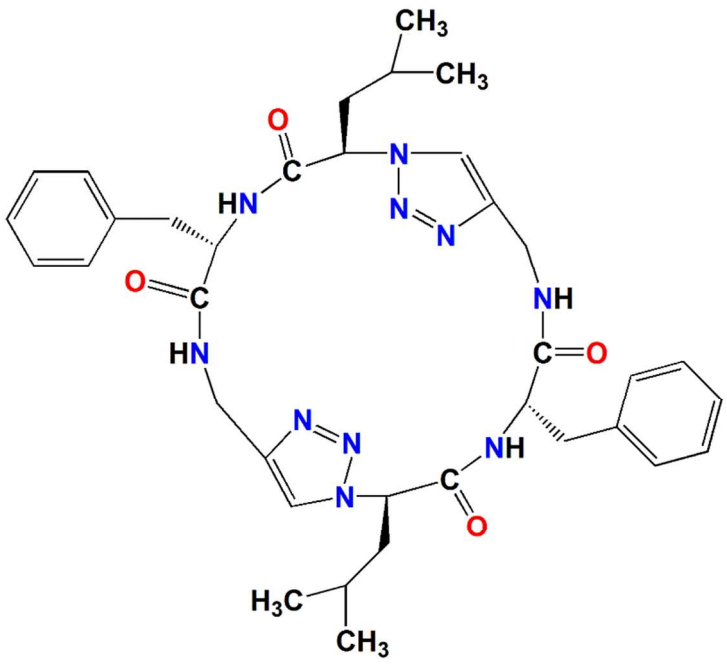

Scheme 1. Single heterocyclic peptide consist of triazol amino acid.

Methods

Molecular dynamic simulations details

The simulated systems will be donated as CPNT and D for the cyclic peptide nanotube and dimer, respectively. The atomic coordinates for the dimer and CPNT were obtained from a previous X-ray crystal structure, which was synthesized by Ghadiri and co-workers.[6] MD has been started on the dimer and CPNT (with/without ethanol as a guest molecule) by energy minimization in an implicit solvent environment to reduce unfavorable short contacts. Each structures (D and CPNT) were solvated with cubic box of water, methanol and chloroform molecules extending 15 Å away from the solute atoms. Water was simulated using the TIP3P

model. Chloroform and methanol models were taken from AMBER parameters.[21-24] Then energy minimization for each structures has been performed for 30000 cycles. After this, each system was heated from 0 to 300 K for 200 ps in a NVT MD simulation (with typical values of restraining force constant of 1000 kJ.mol^{-1}.nm^2 for solute structures). The results of this step were used to start equilibration step for 2000 ps in the NPT ensemble (at 300 K and 1 bar) in the absence of any positional restraints. MD simulation of the products has been performed for 45 ns in the NPT ensemble using a 2fs time step. The Particle Mesh Ewald method (PME) [25] coupled to periodic boundary conditions was used for calculating the long range electrostatic interaction with 8 Å direct space cut-off. In the NPT MD simulation steps, Langvin thermostat [26,27] for controlling the temperature of the system with a collision frequency 2 ps^{-1} and pressure relaxation time of 1 ps was used. Time step of 2 fs was used throughout with SHAKE constraint on all bonds involving hydrogen atoms.[28]

All MD calculations were carried out using AMBER 12.0 simulation software package [29] employing ff12SB force filed [30] and general amber force filed (GAFF) parameters [31] for cyclic peptide derivatives and ethanol as guest molecules, respectively.

MM-PBSA and MM-GBSA calculations

The free energy of binding of each cyclic peptide (CP) unit in a CPNT was calculated using the molecular mechanics-Poisson-Boltzmann surface area (MM-PBSA) and molecular mechanics-Generalized-Born surface area (MM-GBSA) methods as implemented in AmberTools 13.0.[11,32-35] For calculation of the free energies of binding for each CP unit to CPNT, production MD simulation has been performed for 10 ns with the time step of 2 fs for the CPNT with 2 to 8 units of cyclic peptide (minimization, heating and equilibration steps for these CPNTs are as same as conditions that were reported in the simulation details section). The free energy of subunit CP in CPNT was calculated using the equation 1:

$$\Delta G_{binding} = \Delta E_{MM} + \Delta G_{Solv.} - T\Delta S_{solute} \quad (1)$$

Where

$$\Delta E_{MM} = \Delta E_{interal} + \Delta E_{vdW} + \Delta E_{ele} \quad (2)$$

Where in equation 2, $\Delta E_{interal}$, ΔE_{vdW} and ΔE_{ele} represent the internal, vander Waals and electrostatic contribution of molecular mechanics energy, respectively. The solvation energy was calculated by equation 3:

$$\Delta G_{Solv.} = \Delta G_{pol} + \Delta G_{np} \quad (3)$$

Where ΔG_{pol} and ΔG_{np} are the polar and nonpolar contributions of the solvation free energy, respectively. Nonpolar contribution of the solvation free energy was calculated by nonpolar solvation term based on the solvent accessible

surface area (SASA).[11,35] The harmonic approximation of the translational, rotational and vibrational conformational entropies was done using the normal-mode analysis program of MM-PBSA package.[33]

DFT calculations details

The structures of the monomer and dimer of the cyclic peptide, with/without ethanol as guest molecule have been optimized using the M06-2x functional [36] by employing 6-31G(d) basis set [37] as implemented in Gaussian 09 series of program [38]. In order to provide an estimation of the zero point vibrational energies (ZPVEs) as well their corresponding thermochemical parameters, frequency calculations were performed. Since the solvent-solute interactions are more considerable than gas phase, conductor like polarizable continuum model (CPCM) [39,40] has been applied in the presence of methanol, chloroform and water. For investigation of the electronic charge distribution and hydrogen bond (H-bond) formation between the CP units in the dimer structure, natural bond orbital (NBO) analysis was applied.[41] Through the NBO analysis, donor-acceptor interactions between the CP units of the dimer have been studied. Finally, the topological properties,[42,43] electron location function (ELF) [44-50], localized orbital locator (LOL)[51,52] and atoms in molecules (AIM) [42] analyses were performed using the MultiWFN 3.1.[53]

Results and discussion

MD simulation results

Dynamical properties of the dimer

The stability of the dimer is determined by the intermolecular H-bond interaction between NH and CO (NH···O=C) groups. The nature of the solvents from the molecular view point can influence the power of H-bond interaction between the CP units of the dimer. For this purpose, the effect of water (polar), methanol (medium polarity) and chloroform (nonpolar) was studied. Root mean square deviation (RMSD) values of the heavy atoms of CP untints were calculated, with respect to the initial geometry from the MD trajectories (Figure 1-A). According to RMSD values, it reveals that the dimer is lees stable in water because the maximum of the RMSD is in water. Moreover, dimers in the polar and medium polar solvents have more fluctuations in comparison to nonpolar solvent. Analysis of the radii of gyration (Rg) of the CP units (Figure 1-B) in different solutions, shows that distances between the CP units of dimer in chloroform is lower than water and methanol. Because larger Rg shows that dimer structure is lees compact in water and methanol. The average distance between N and O atoms of CP units after 45 ns of the MD simulations, in water, methanol and chloroform are 3.04, 3.03 and 2.84 Å, respectively. Dimer structures after 45 ns of the MD simulation

are shown in Figure 2. According to Figure 2, the dimer in chloroform has cylindrical structure, which is not true in water.

According to calculation, there are six hydrogen bonds between the two monomers of CP in chloroform with is higher than methanol and water (Figure S1). Average hydrogen bond length of (NH···O=C) is 1.9 Å in chloroform which is slightly smaller than in water (2.10 Å) and methanol (1.98 Å). Larger number of the H-bond and its shortness in chloroform, are reasons for lower RMSD value of the dimer structure in this solvent. Higher RMSD values of the dimers in methanol and water, may be interpreted by the competition between the NH of the CP and OH of the waters and methanol molecules with C=O groups of the CP monomers for the H-bond formation. The competition between intersubunit H-bonding and H-bonding with water molecules has also been reported, previously.[54]

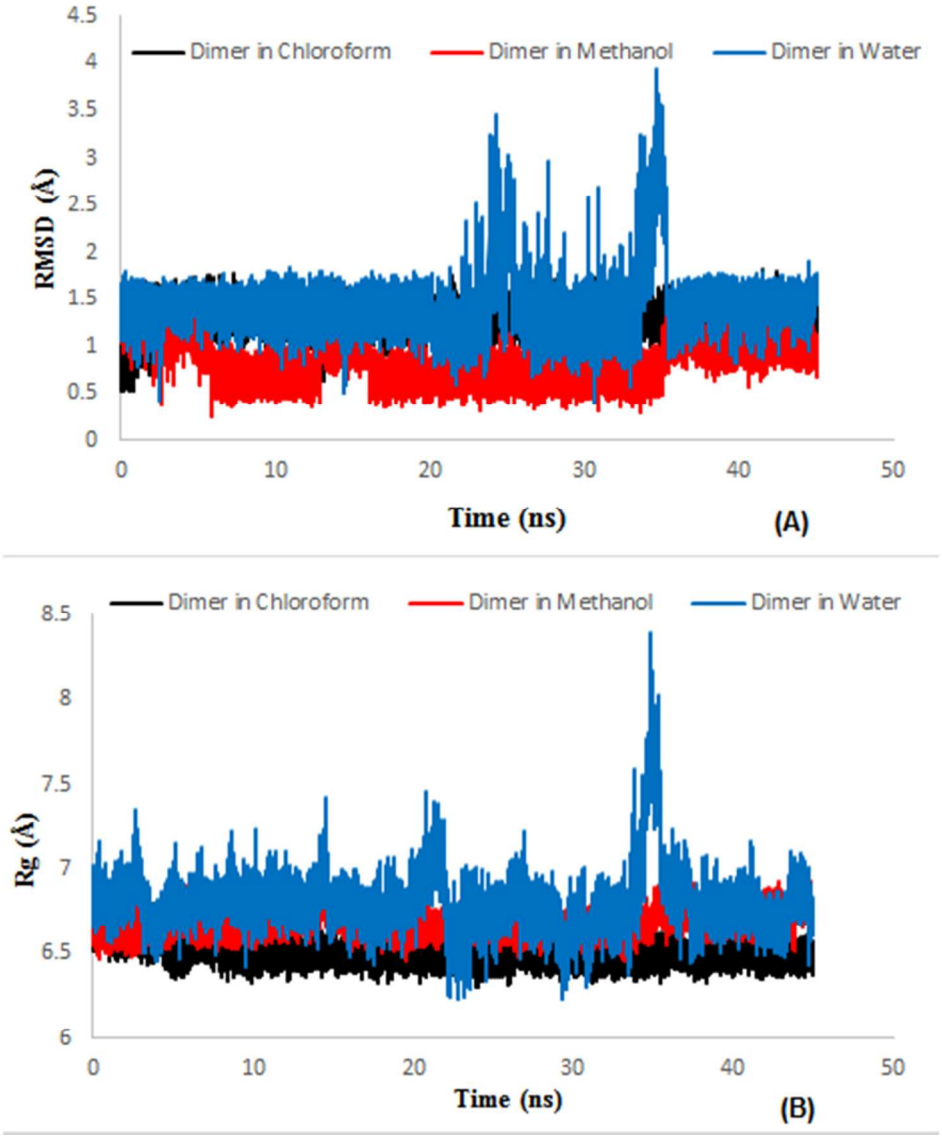

Figure 1. Calculated RMSD (A) and Rg (B) values in (Å) of the dimer as a function of time during 45 ns MD simulations in water, methanol and chloroform.

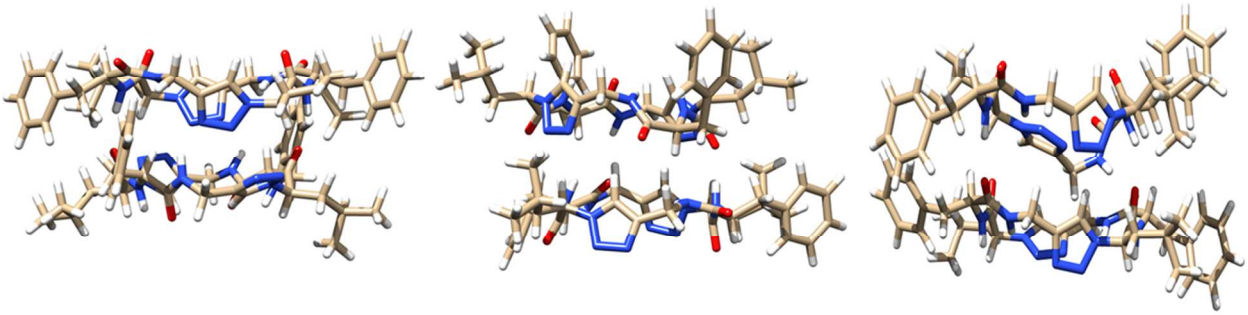

Figure 2. Obtained dimer structures after 45 ns of the MD simulation in chloroform, methanol and water (from the left to right).

Figure 3 represents the partial radial distribution function of O···H pairs (C=O···HN) of the dimer in chloroform, methanol and water. This figure shows the probability of finding a pair of O···H atoms in term of intermolecular distances. According to Figure 3, the behavior of the dimer in the studied media is completely different. The first peak in chloroform and methanol is at r=1.85 Å. This peak is related to the O···H distance and confirmed the H-bond formation between the CP monomers of dimer.

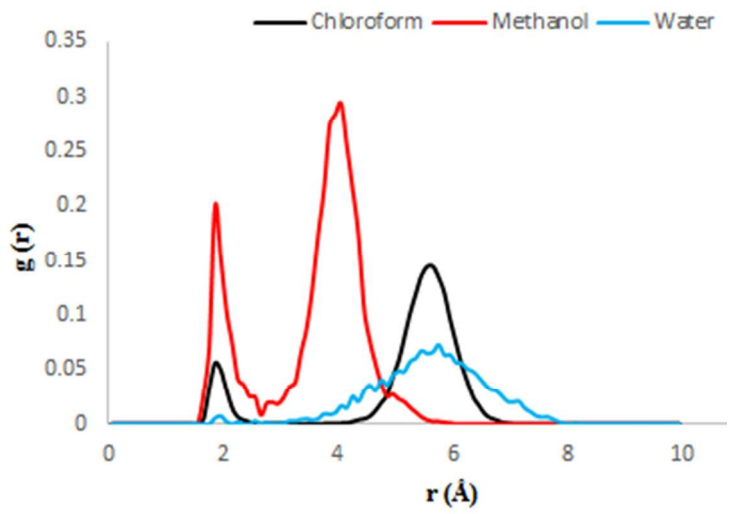

Figure 3. RDFs between the O and H atoms of the CP dimer in different solvents.

Dynamical behavior of the CPNT in methanol, Chloroform and water

In order to investigation the studied parameters on the length of the cyclic peptide nanotube, MD simulation on CPNT consist of eight monomers in methanol, chloroform and water have been performed. Figure 4-A shows the corresponding calculated RMSD values of the CPNT in different solvents. Although RMSD values are enough low, showing the stability, but RMSD values were increased in comparison to the Dimer. CPNT-solvent interaction as a function of the solvent polarity is similar to the dimer. Analysis of Rg of the CPNT (Figure 4-B) reveals that the CPNT in water is more compact than chloroform and methanol, which is in contrast to dimer. Considering the number of intermolecular H-bond (Figure S2), reveals that CPNT in chloroform has the maximum number of H-bond (42) in the most snapshots obtained of the trajectories of 45 ns in the MD

simulation. Since there are number of the H-bond in chloroform, it has the lowest value of RMSD and more stable in this solvent.

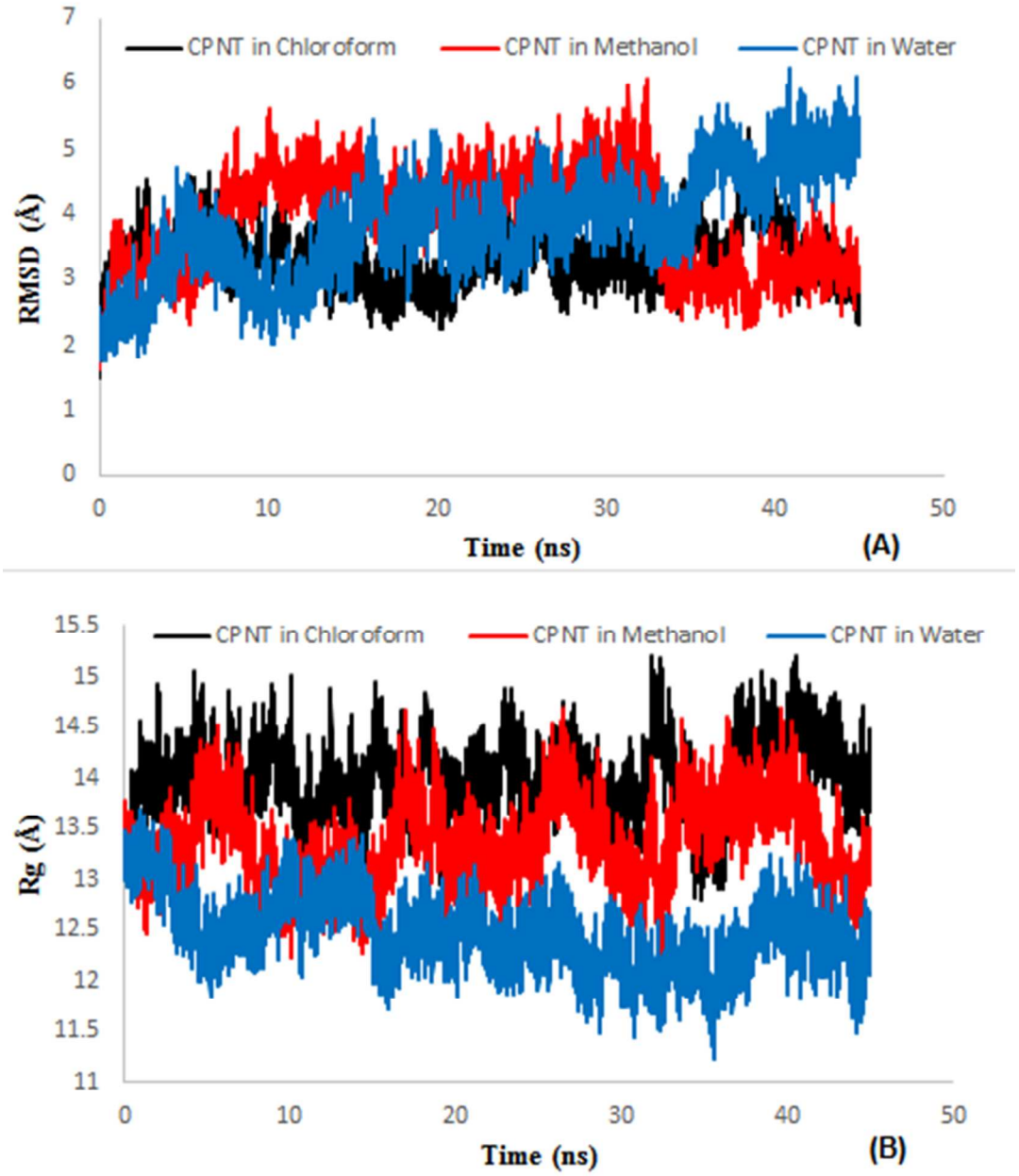

Figure 4. Calculated RMSDs (A) and Rg (B) of CPNT in chloroform, methanol and water.

The effect of the guest molecule on the stability of the dimer and CPNT

Obtained X-ray crystallography data on the CP structure by Ghadiri and co-workers [6] in ethanol indicated that the peptide subunit adapt the expected flat ring shape conformation and stack in parallel fashion in to tubular assemblies with ordered ethanol molecules filling the channel pores.[6] Therefore, the investigation of ethanol effects as a guest molecule on the stability of dimer and CPNT structures is of importance from the molecular approach.

To investigate the effect of guest molecule, one and seven ethanol molecule in the cavity of dimer and CPNT are inserted, respectively and these structures were immersed in the box of water, chloroform and methanol during the MD simulations, described previously. Calculated RMSD values (Figure 5-A) for the dimer including ethanol the presence of three solvents is lower than dimer without ethanol indicating that the guest molecule makes the dimer stable in polar and nonpolar solvents. Rg analysis confirms the results of RMSD, too (Figure 5-B) confirming lower fluctuation in comparison to dimer without ethanol. In these conditions, the number of H-bonds is increased (7 in chloroform and 6 in water and methanol) according to figure S3, makes the CP more stable. Figure 6 shows the obtained the dimer structures with e guest molecule from 45 ns MD simulations.

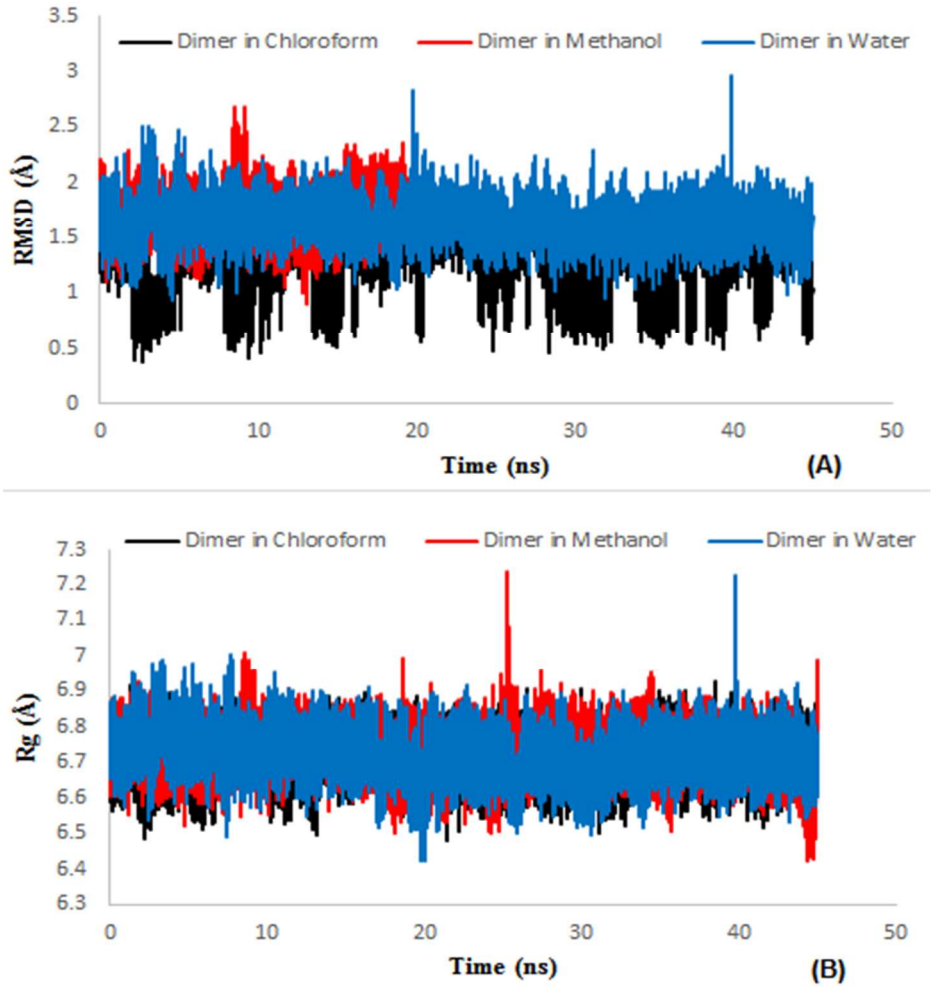

Figure 5. RMSD (A) and Rg (B) of the dimer with a guest molecule of ethanol in water, chloroform, and methanol.

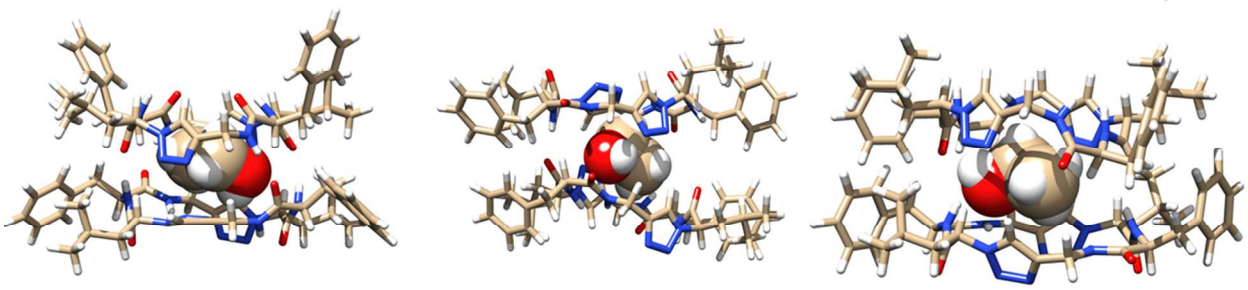

Figure 6. Obtained dimer structures after 45 ns of MD simulations with guest molecule in chloroform, methanol and water (from left to right).

Figure 7-A shows the calculated radial distribution function for C=O····HO pair (O atom of CP unit and H atom of ethanol molecule inside the dimer). According to this figure, the first sharp peaks observed in methanol and chloroform being centered at r=1.85 and 1.75 Å, respectively, confirming H-bond formation between the CP units of the dimer and guest molecule. Figure 7-B represents the calculated radial distribution function for HO····HN pair (O atom of ethanol and H atom of CP units of the dimer). According to this figure the first sharp peak obtained in water and methanol at 2.05 Å, reveals that the H-bond formation between O atom of CP and H atom of guest molecule is more stable than H-bond formation between the O atom of guest molecule and H atom of CP. There are two remarkable points: firstly interaction between O atom of ethanol and H atom of CP has not been observed in chloroform according to Figure 7-B and the second, comparison of Figures 7-A and B reveals that the solvents affect the interactions of CP units of the dimer by the guest molecule.

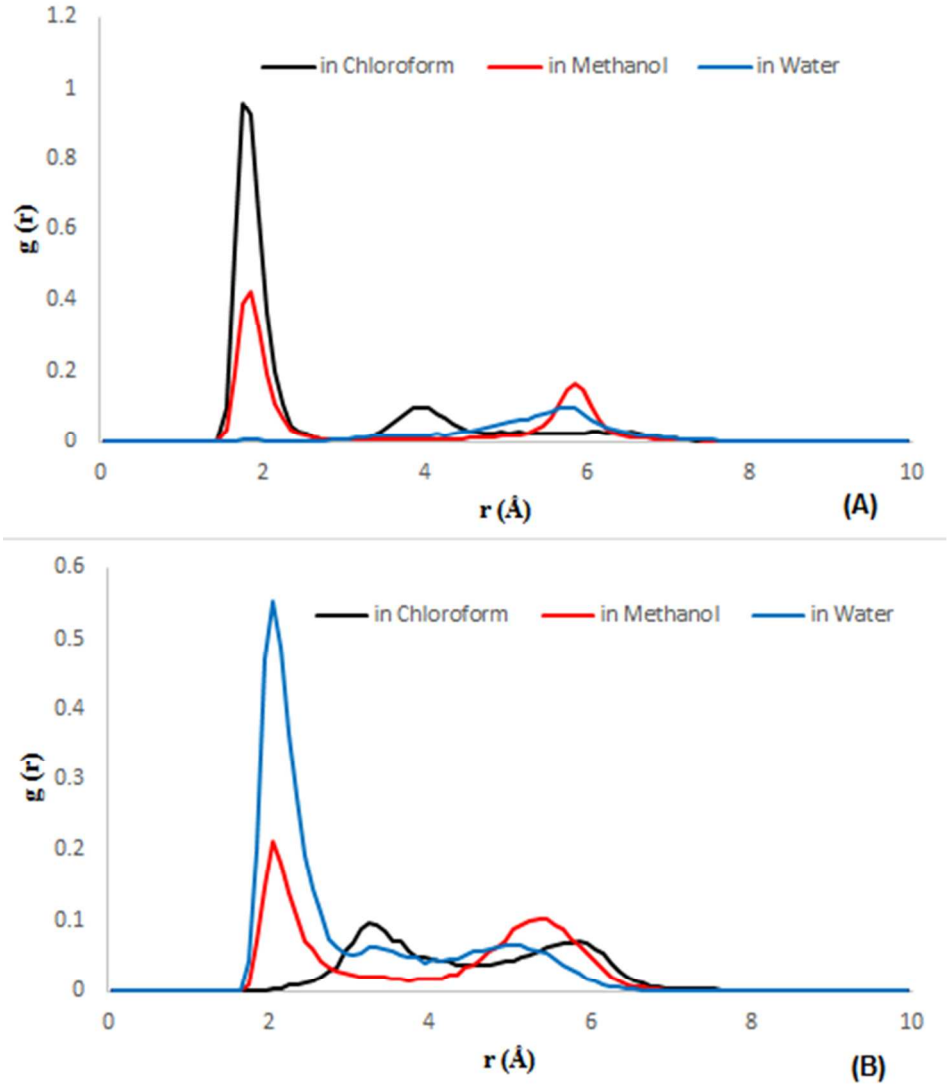

Figure 7. Calculated RDF of O···H pair in water, methanol and chloroform. (A) O atom of CO group of CP with H atom of OH group of ethanol and (B) O atom of OH group of ethanol with H atom of NH group of CP units of dimer.

Seven ethanol molecules inserted in the CPNT, one ethanol for two CPs and immersed into the boxes of methanol, water and chloroform. RMSD values (Figure S4-A) of the systems at this conditions reveal that the CPNT is more stable with guest molecules (1.5 1.6 and 1.8 Å in chloroform, methanol and water,

respectively) than pure CPNT. Rg analysis (Figure S4-B) confirms the results of the RMSD calculations. Figure 8 shows the CPNT with guest molecules after 45 ns of MD simulations in water. Radial distribution function analysis of O···H pair of the guest molecules and CPNT shows that the guest molecules have different behavior in CPNT structure in comparison to the dimer.

Figure 9-A shows the radial distribution function (RDF) of O···H pair (O atom of ethanol and H atom of CPNT). According to this figure, O atom of OH group (in ethanol) is 2.25 Å far from H atom of NH groups (in CPNT) in methanol and water, while this distance in dimer is 2.05 Å. Calculated RDF for O···H pair (O atoms of CPNT and H atom of OH group of ethanol) in Figure 9-B shows that the corresponding distance is 2.15 Å in all solvents. These results indicate that solvents do not affect the interaction between guest molecules and CP units of the CPNT. More analysis shows that ethanol molecules have intermolecular hydrogen bond with other ethanol molecules inside the CPNT. H-bond formation between the guest molecules and CP unites of the CPNT have not been observed in these solvents. It confirms that behavior of guest molecule in the dimer is completely different in comparison to the CPNT.

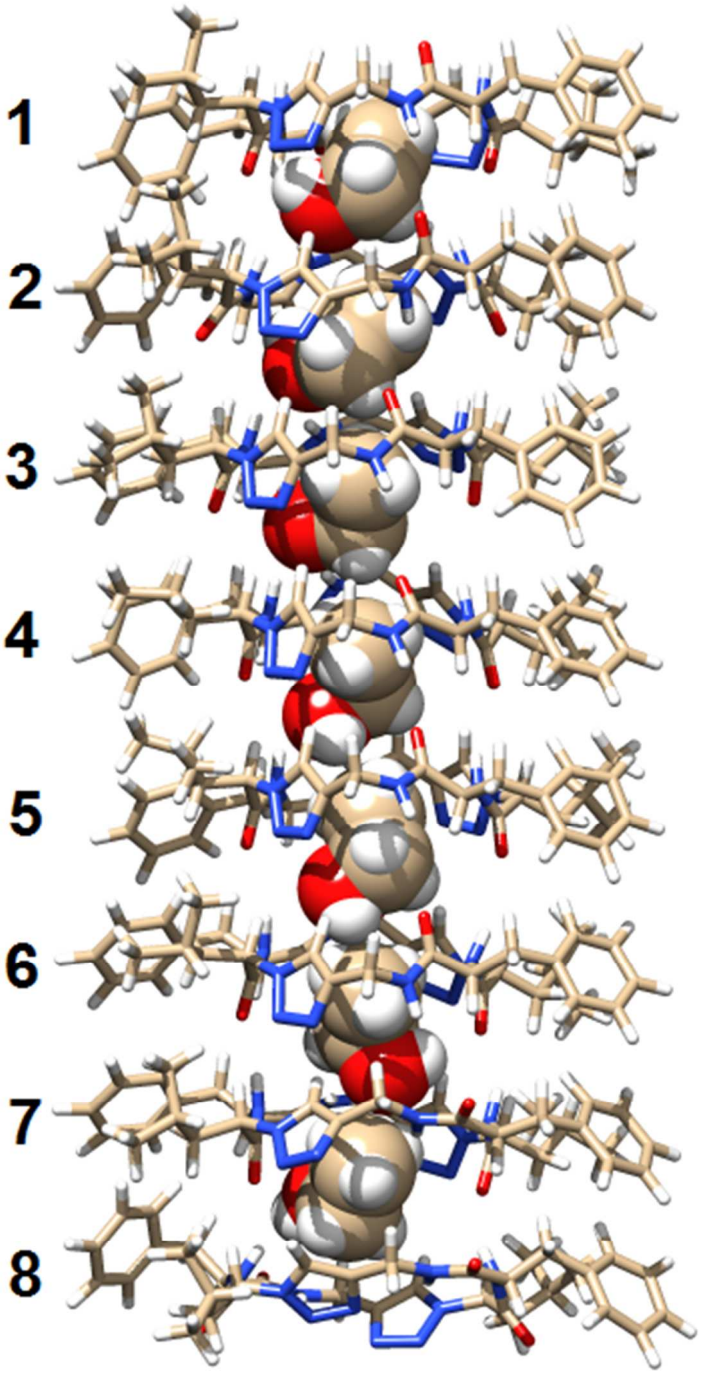

Figure 8. CPNT with guest molecules after 45 ns of MD simulations in water.

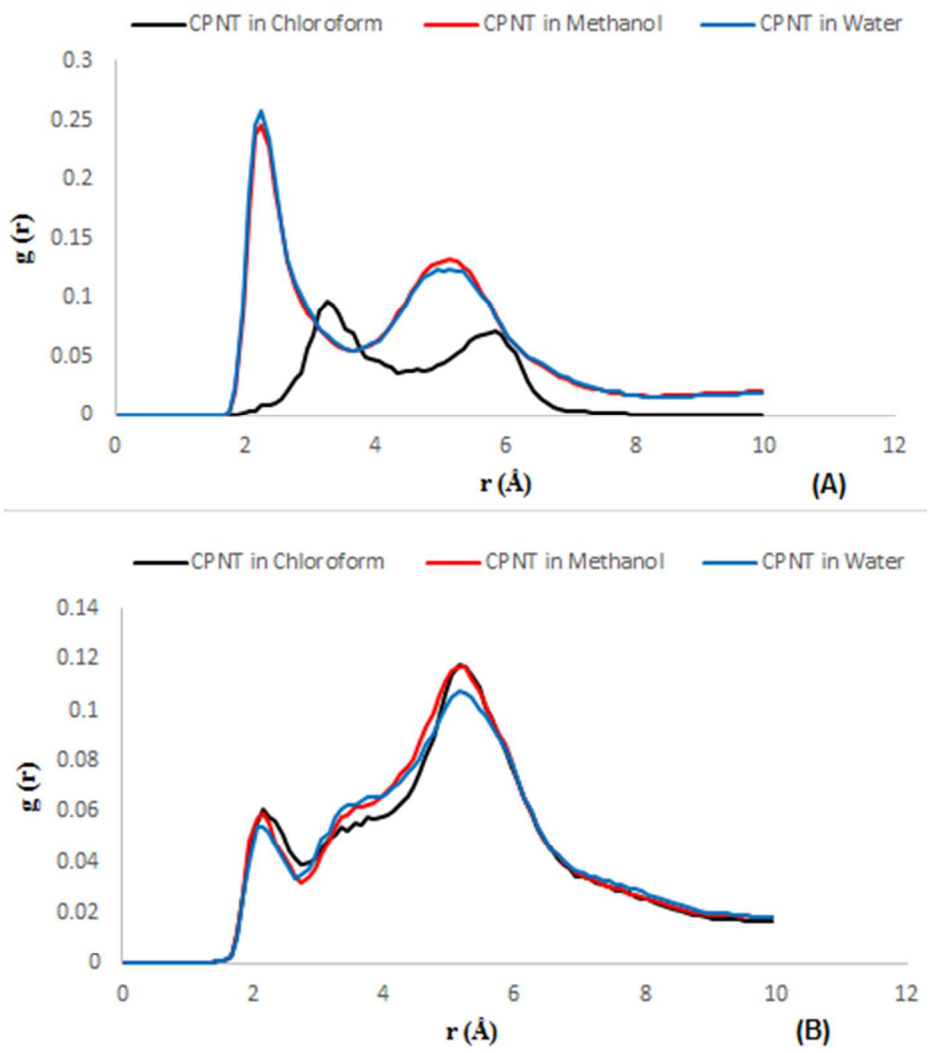

Figure 9. RDF diagrams of O···H pair in different solvents. (A) H atom of the CPNT (NH groups) with O atom of the ethanol (OH group) and (B) H atom of the ethanol (OH group) with O atom of the CPNT (CO groups).

Calculated free energy of binding

Calculated contributions of the free energy of binding from Poisson-Boltzmann (PB) method are reported in Table 1. According to Table 1, Van der Waals energy of the self-assembling process is the highest in chloroform, the solvent which has the highest hydrophobic interactions with CPNT. The

contribution of the electrostatic energy (ΔE_{ele}) in water is more than chloroform and methanol, because of many H-bond interactions with CPNT. Polar solvents such as water and methanol reduces the nonpolar contributions of the free energy of binding. Calculated total entropies confirmed the self-assembling process in different solvents. Data analysis reveals that increase in the length of the CPNT in Chloroform elevates the solvation Gibbs free energy (ΔG_{sol}).

Table 1. Calculated contributions of the energy components (kcal.mol^{-1}) for step by step CP addition PB method in different solvents.

				Water			
	CP2	**CP3**	**CP4**	**CP5**	**CP6**	**CP7**	**CP8**
ΔE_{vdW}	-22.41	-24.99	-26.46	-25.06	-25.43	-25.18	-24.17
ΔE_{ele}	-4.63	-5.26	-8.45	-7.73	-7.41	-7.11	-7.51
ΔE_{PB}	8.19	9.05	11.04	10.38	10.16	10.19	10.31
ΔE_{np}	-18.89	-19.69	-20.47	-20.07	-20.01	-19.61	-19.29
ΔG_{gas}	-27.04	-30.25	-34.91	-32.80	-32.84	-32.29	-31.69
ΔG_{sol}	19.13	21.13	23.17	22.32	22.23	22.55	22.40
ΔS_{tot}	-20.39	-20.20	-20.05	-18.99	-19.89	-20.19	-19.92
				Methanol			
	CP2	**CP3**	**CP4**	**CP5**	**CP6**	**CP7**	**CP8**
ΔE_{vdW}	-22.32	-23.15	-23.26	-23.69	-23.50	-22.02	-22.44
ΔE_{ele}	-6.26	-6.96	-7.74	-6.98	-7.09	-7.42	-8.10
ΔE_{PB}	8.36	9.47	9.75	9.64	9.67	9.81	10.32
ΔE_{np}	-18.97	-19.19	-19.72	-19.84	-19.51	-18.54	-18.88
ΔG_{gas}	-28.58	-30.10	-31.00	-30.67	-30.59	-29.44	-30.54
ΔG_{sol}	19.24	21.41	21.61	21.36	21.62	22.12	22.24
ΔS_{tot}	-20.32	-20.14	-19.73	-19.28	-19.11	-20.01	-19.92
				Chloroform			
	CP2	**CP3**	**CP4**	**CP5**	**CP6**	**CP7**	**CP8**
ΔE_{vdW}	-23.58	-26.02	-25.43	-25.06	-26.78	-24.91	-24.62
ΔE_{ele}	-6.38	-6.93	-6.70	-8.06	-8.58	-8.04	-7.76
ΔE_{PB}	6.24	6.70	6.74	7.10	7.25	7.37	7.22
ΔE_{np}	-19.76	-20.01	-19.91	-19.68	-20.84	-19.74	-19.49
ΔG_{gas}	-29.96	-32.95	-32.12	-33.12	-35.36	-32.95	-32.39
ΔG_{sol}	16.94	18.69	18.52	19.21	19.25	19.41	19.26
ΔS_{tot}	-19.70	-20.46	-19.56	-20.08	-20.14	-20.36	-19.34

Calculated total free energies of binding by PB and GB methods with their standard deviation (SD) for the self-assembling process were reported in Table 2. According to data, the length of the peptide nanotube can be controlled by the solvent polarity. Calculated total free energy of binding in chloroform is more than in methanol and water, because the highest number of the H-bonds in CPNT are in chloroform. Linear correlation of the number of CP and total free energy are depicted in Figure 10. According to this figure, hexamer of the CPNT in chloroform is the most stable tube at the both methods of PB and GB.

Table 2.Calculated total free energy of binding (kcal.mol^{-1}) for addition of CP unit to other CP units in different solvents by PB and GB methods.

PB method						
	Water		Methanol		Chloroform	
Number of CP units	ΔG	SD	ΔG	SD	ΔG	SD
2	-7.91	2.16	-9.34	2.18	-13.03	2.39
3	-9.12	2.35	-8.69	2.33	-14.26	2.13
4	-11.74	3.03	-9.40	2.25	-13.61	3.53
5	-10.48	2.40	-9.31	2.92	-13.91	2.96
6	-10.60	1.97	-8.96	2.34	-16.11	2.88
7	-9.74	2.12	-7.31	2.52	-13.54	2.40
8	-9.29	1.95	-8.31	2.67	-13.13	1.87
GB method						
	Water		Methanol		Chloroform	
Number of CP units	ΔG	SD	ΔG	SD	ΔG	SD
2	-23.21	2.27	-23.65	2.20	-24.76	2.35
3	-25.89	2.13	-24.38	1.88	-27.45	1.99
4	-27.93	2.82	-24.64	2.62	-26.68	3.00
5	-26.34	2.19	-24.97	2.88	-26.32	2.65
6	-26.60	1.77	-24.66	2.37	-28.35	2.74
7	-26.31	2.16	-23.20	2.52	-26.36	1.98
8	-25.34	2.05	-23.68	2.45	-26.10	1.90

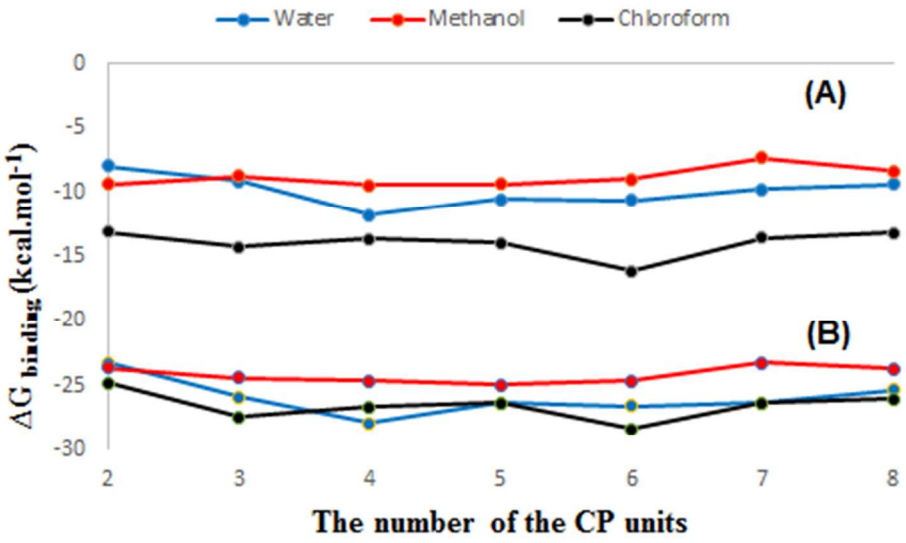

Figure 10. Relationship between the number of CP and calculated total free energy of binding by the PB method (A) and GB method (B).

Structural, IR vibrational frequencies and energy analysis by DFT method

Optimized structures of the CP monomer, dimer and dimer/guest molecule, with atom numbering are shown in figures S5, S6 and S7. Structural parameters obtained from theoretical and experimental results are summarized in Table S1. According to Table S1, theoretical results are in good agreement with the experimental dada.[6] C=O and N—H bond lengths in the dimer structure are bigger than monomer because of H-bond formation (C=O···H—N). Moreover, calculated O···H distances are lower than experimental data. Average calculated angle of

NCO is around 123° and the experimental value is 125°, showing that for the current purposes, the results derived from the M06-2X/6-31G(d) level will be suffice.

Electronic density of states (DOS) for the monomer and dimer of CP and the corresponding band gaps were depicted in Figure S8. Comparison between the calculated band gaps of the monomer and dimer reveals that dimerization process reduces HOMO-LUMO energy level (Figure S9). Nonpolar solvent decreases the band gap both of the monomer and the CP dimer. Band gap of this cyclic peptide system is greater than the standard semiconducting materials. However the features of an open-ended hollow tubular structures, implies that this material can be packed inside to obtain a variety of molecular electronic devices.[55] In addition to self-assembling, inclusion complex of the guest molecule (ethanol) reduces the band gap. For example the band gap of the dimer in the gas phase and water are 8.36 and 8.79 eV, while for the inclusion complex in the gas phase and water are 8.26 and 8.76 eV, respectively.

Calculated IR vibrational frequencies of C=O and N—H bonds of CP monomer and dimer are reported in Table S2. N—H vibrational stretching modes of the monomer are 3641 and 3633 cm^{-1} and of dimer structure are 3565, 3650, 3497 and 3529 cm^{-1} in the gas phase. These fluctuations are due to hydrogen bonding in CP dimer. C=O stretching modes of the CP monomer in the gas phase are 1845 and 1815 cm^{-1} while for the CP dimer are 1818, 1850, 1754 and 1773 cm^{-}

[1]. Calculated vibrational frequencies of N—H and C=O bonds of monomer show blue and red shift, respectively, in methanol, chloroform and water in comparison to gas phase. The effect of solvents on the IR vibrational frequencies, based on the solvent polarity, have been observed in our previous studies.[56,57] According to Table S2, calculated IR vibrational frequencies for the dimer of N—H bond have both red and blue shift while for C=O bonds only red-shift have been observed in solution in comparison to gas phase.

Gibbs free energies of dimerization have been calculated in the gas and solution phases. Calculated Gibbs free energies by DFT method are higher than those of the molecular mechanics method. Gibbs free energies of dimerization are -33.67, -18.80, -18.53 and -19.16 kcal.mol^{-1}, in gas phase, water, chloroform and methanol, respectively. Each H-bond (C=O$^{\cdots}$H—N) has interaction energy, 35.21, 19.66, 19.38 and 20.04 kJ.mol^{-1}, in the gas, water, chloroform and methanol, respectively. Which are close to the commonly accepted value (20 kJ.mol^{-1}) for a typical hydrogen bond in solution.

Although the calculated value in the gas phase (35.21 kJ.mol^{-1}) is higher than 20.00 kJ.mol^{-1} but the obtained data in solutions are close it. These results strongly confirm the formation of C=O$^{\cdots}$H—N hydrogen bond in the dimer which is the primary driving force in stabilizing the CP dimer. Moreover Gibbs free energy of formation for the inclusion complex in the water and gas phase have

been calculated. Inclusion of ethanol molecule inside the CP dimer increases the Gibbs free energy of formation by -8.63 (-27.43) and -9.71 kcal.mol^{-1} (-43.38) in the gas and (water), respectively. This means that ethanol stabilized the CP dimer, which is in agreement with the MD simulation results.

AIM analysis

Quantum theory of atoms in molecules (QTAIM) analysis on the CP dimer for investigation H-bond interaction was performed at the M06-2X/6-31G(d). In this analysis, chemical bonding can be characterized by a so-called bond critical point (BCP). BCP properties of O···H in the CP dimer have been calculated in the gas and solution phases and reported in Table 3. The electron density (ρ) of the BCP shows the bond strength, because larger value of electron density reveals grater interaction energy.

According to Table 3, calculated values of ρ for O···H bond shows that the O···H interaction in the solution is more than gas phase. According to Table 3, calculated values of $\nabla^2(\rho)$ for O126···H82 and O78···H172 are negative in different solvents, showing the H-bond formation. Also, the ratios of –G/V for all O···H interactions are more than 1.0 showing the non-covalent character. Analysis of the H (G+V) values, shows that total energy density of O126···H82 in the gas phase and O78···H172 in chloroform are positive, confirming O···H interaction has

electrostatic character. Moreover electron location function (ELF) and localized-orbital locator (LOL) of O···H bonds have been analyzed and shown in Figure 11. A large value of ELF means that electrons are greatly localized, indicating covalent bond, alone pair or inner shells of an atom involved.

According to Figure 11 the values of ELF and LOL in the regions between the O and H atoms in the gas phase are low, showing the electrostatic interactions between these atoms in the CP dimer. Similar calculations on the inclusion dimer with ethanol show that the guest molecule introduces electrostatic interactions with CP dimer, in the gas phase and water.

Table 3. Calculated topological properties of O···H bonds at the BCP in the gas phase and different solvents for the CP dimer.

bond	parameters	Gas	Water	Methanol	Chloroform
	ρ	0.0193	0.3110	0.3193	0.3102
O126···H82	$\nabla^2(\rho)$	0.0702	-0.8447	-1.6026	-0.8448
	-G/V	1.0232	0.2432	0.0835	0.2431
	ρ	0.0277	0.2375	0.2679	0.0052
O78···H172	$\nabla^2(\rho)$	0.1043	-0.5190	-0.8920	0.0170
	-G/V	1.1953	0.2309	0.1258	1.3475
	ρ	0.0181	0.4038	0.0069	0.0262
O146···H48	$\nabla^2(\rho)$	0.0670	0.3323	0.0245	0.0880
	-G/V	1.0271	0.5289	1.2686	0.9754
	ρ	0.0264	0.0182	0.0030	0.0182
O1···H100	$\nabla^2(\rho)$	0.0877	0.0666	0.0132	0.0667
	-G/V	0.9728	1.0220	1.5352	1.0240

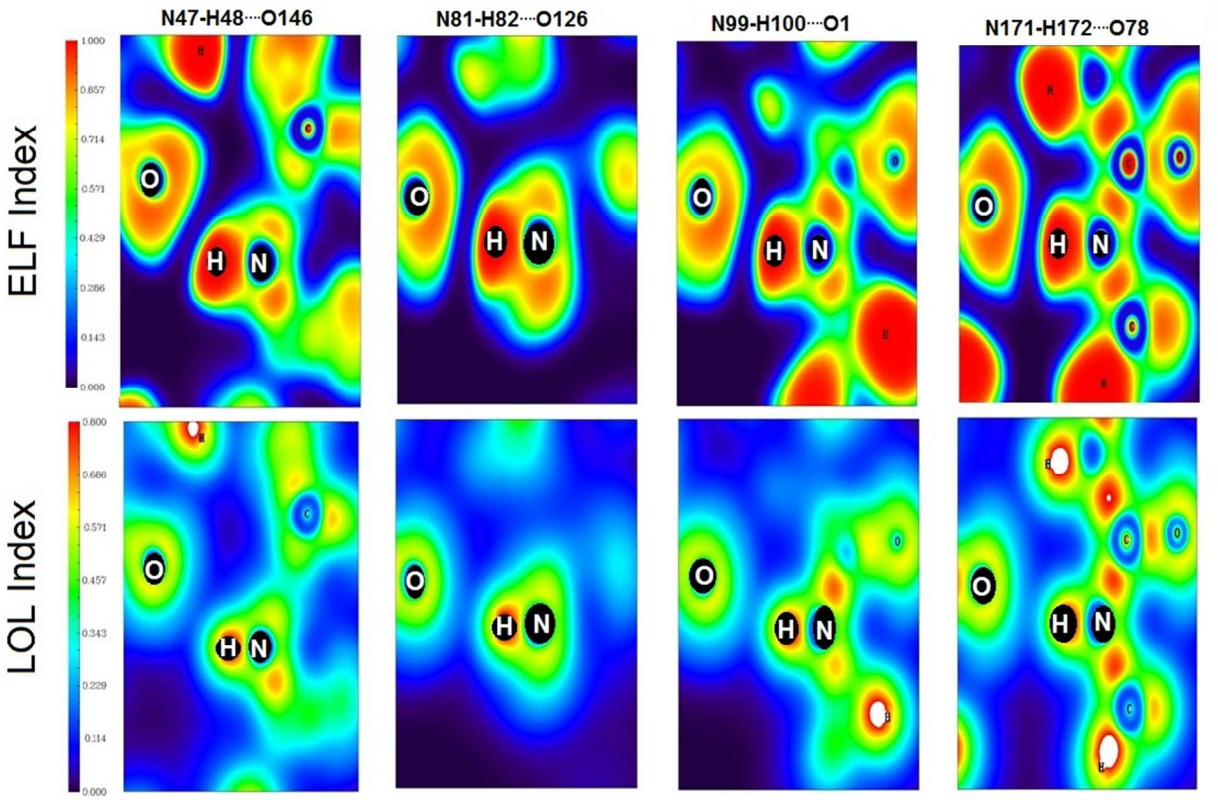

Figure 11. Electron location function (ELF) and localized orbital locater (LOL) of O···H bonds of the CP dimer in the gas phase.

NBO analysis

Natural atomic charges through the NBO analysis have been calculated and reported in Table 4. According to this, table negative electronic charge of O atoms and positive character of H atoms have been increased during the dimerization. These changes show O···H interaction between the CPs in the dimer. Comparing the atomic charges in the gas phase and different solvents, reveals that solvents affect the H-bond formation between the two CPs in the dimer.

In order to have a comprehensive understanding of the interactions during the dimerization, donor-acceptor orbital interactions have been calculated and reported in Table 5. In this table, large stabilization energies is due to the strong orbitals interactions between the lone pair of O atoms and antibonding molecular orbitals of N—H bonds ($\sigma^*_{N—H}$). Water and methanol reduce the interactions between the lone pairs of O78 and O1 atoms with $\sigma^*_{N171—H172}$ and $\sigma^*_{N99—H100}$, respectively. While the interaction energy between the lone pairs of O126 and O146 atoms with $\sigma^*_{N81—H82}$ and $\sigma^*_{N47—H48}$ are increased respectively. According to $\sum E(2)$ values, there are highest perturbation effects in chloroform between the two CPs of the dimer in comparison to other solvents. Therefore, the CP dimer is more stable in the nonpolar solvent than methanol and water. This result is accordance to MD simulations.

Table 4. Natural atomic charges of some atoms involved in O····H bond of CPs monomer and dimer in the gas phase and different solvents.

Atoms	Structures	Gas	Water	Chloroform	Methanol
O1	Monomer	-0.6668	-0.6859	-0.6824	-0.6856
	Dimer	-0.7232	-0.7186	-0.7204	-0.7188
H48	Monomer	0.4416	0.4535	0.4505	0.4533
	Dimer	0.4578	0.4652	0.4612	0.4624
O78	Monomer	-0.6665	-0.6856	-0.6820	-0.6853
	Dimer	-0.7307	-0.7276	-0.7291	-0.7777
H82	Monomer	0.4416	0.4536	0.4506	0.5433
	Dimer	0.4485	0.4526	0.4514	0.4525

Table 5. Significant natural bond orbital interactions between the two CPs in the gas phase and different solvents and their second-order perturbation stabilization energies E(2) (kcal.mol^{-1}).

	Gas	Water	Chloroform	Methanol
$Lp_{O126} \rightarrow \sigma^*_{N81—H82}$	8.79	9.01	8.96	9.01
$Lp_{O78} \rightarrow \sigma^*_{N171—H172}$	14.69	14.50	14.56	14.51

$Lp_{O146} \rightarrow \sigma^*_{N47—H48}$	5.18	5.33	5.28	5.31
$Lp_{O1} \rightarrow \sigma^*_{N99—H100}$	13.26	12.95	13.03	12.96
$\sum E(2)$	7352.40	7024.18	7598.07	7024.23

Conclusion

45 ns molecular dynamic simulations on the CPNT and cyclic peptide dimer in methanol, water and chloroform shows that these structures are more stable in nonpolar solvent. Rg and RMSD calculations of these structures reveal that CPNT and cyclic peptide dimer in chloroform have the lowest fluctuation showing its stability. Additionally, the competition between intersubunit H-bonding and H-bonding with molecules of water and methanol destabilized the CPNT and CP dimer in polar solvents.

MM-PBSA and MM-GBSA data reveal that the CPNT composed of 6 CP units is the stable in chloroform. Calculated step by step free energy of binding for CP addition confirmed that all CPNTs composed of 1 to 8 units are stable in chloroform in comparison to other solvents. This means that solvents have key role on the stability and the length of the CPNT. Analysis of intersubunit H-bonds of the CP dimer and CPNT shows that there are highest numbers of H-bond in chloroform which in turn stabilizes the CPNT.

NBO analysis of the H-bond between two units of the dimer, reveals that two CPs have the highest interactions in chloroform. According to calculated Gibbs free energies, CP dimer is more stable in the gas phase than in different

solvents. AIM analysis confirmed that guest molecule inside the dimer stabilized the CP dimer by electrostatic interactions with CP dimer in the gas phase and water.

Acknowledgement

Research council of Ferdowsi University of Mashhad is acknowledged for financial supports (Grant No. 2/32474, 1393/10/9).

References

1 M. R. Ghadiri, J. R Granja, R. A. Milligan, D. E. McRee, N. Khazanovich, *Nature,* 1993, 366, 324.
2 D. Seebach, J. L. Matthews, A. Meden, T. Wessels, C. Baerlocher, L. B. McCusker, *Helv. Chim. Acta*, 1997, 80, 173.
3 T. D. Clark, L. K. Buehler, M. R. Ghadiri, *J. Am. Chem. Soc*., 1998, 120, 651.
4 M. Amorin, L. Castedo, J. R. Granja, *J. Am. Chem. Soc*., 2003, 125, 2844.
5 J. H. V. Maarseveen, W. S. Horne, M. R. Ghadiri, *Org. Lett*., 2005, 7, 4503.
6 W. S. Horne, C. D. Stout, M. R. Ghadiri, *J. Am. Chem. Soc*., 2003, 125, 9372.
7 C. A. Mirkin, *Small*, 2005, 1, 14.
8 C. R. Martin, P. Kohli, *Nat. Rev. Drug Discovery*, 2003, 2, 29.
9 R. Vijayaraj, S. V. Damme, P. Bultinck, V. Subramanian, *Phys. Chem. Chem. Phys*., 2013, 15, 1260.
10 R. Vijayaraj, S. V. Damme, P. Bultinck, V. Subramanian, J. Phys. Chem. B, 2012, 116, 9922.

11 R. Vijayaraj, S. V. Damme, P. Bultinck, V. Subramanian, *Phys. Chem. Chem. Phys*., 2012, 14, 15135.

12 D. T. Bong, T. D. Clark, J. R. Granja, M. R. Ghadiri, *Angew. Chem., Int. Ed*., 2001, 40, 988.

13 Special issue on supramolecular chemistry and self-assembly, *Science,* 2002, 295, 2395.

14 R. R. Ketchem, W. Hu, T. A. Cross, *Science*, 1993, 261, 1457.

15 D. A. Langs, *Science*, 1988, 241, 188.

16 H. Hamada, S. Matsunaga, G. Yano, N. Fusetani, *J. Am. Chem. Soc*., 2004, 127, 110.

17 S. Matile, A. Vargas Jentzsch, J. Montenegro, A. Fin, *Chem. Soc. Rev.* 2011, 40, 2453.

18 C. Valery, M. Paternostre, B. Robert, T. Gulik-Krzywicki, T. Narayanan, J. C. Dedieu, G. Keller, M. L. Torres, R. Cherif-Cheikh, P. Calvo, F. Artzner, *Proc. Natl. Acad. Sci. U. S. A.,* 2003, 100, 10258.

19 K. Namba, R. Pattanayek, G. Stubbs, M. Engels, *J. Mol. Biol.,* 1989, 208, 307.

20 D. Hford, M. R. Ghadiri, *J. Am. Chem. Soc,.* 1995, 117, 9151.

21 W. L. Jorgensen, *J. Am. Chem. Soc*., 1981, 103, 335.

22 W. L. Jorgensen, J. Chandrasekhar, J. D. Madura, R. W. Impey, Klein, M. L., *J. Chem. Phys.,* 1983, 79, 926.

23 P. Cieplak, J. Caldwell, P. Kollman, *J. Comput. Chem*., 2001, 22, 1048.

24 J. Wang, W. Wang, P. A. Kollman, D. A. Case, *J. Mol. Graphics Modell*., 2006, 25, 247.

25 U. Essman, L. Perera, M. Berkowitz, T. Darden, H. Lee, L. Pedersen, *J. Chem. Phys.*, 1995, 103, 8577.

26 B. P. Uberuaga, M. Anghel, A. F. Voter, *J. Chem. Phys.,* 2004, 120, 6363.

27 D. J. Sindhikara, S. Kim, A. F. Voter, A. E. Roitberg, *J. Chem. Theory Comput.,* 2009, 5, 1624.

28 J. P. Ryckaert, G. Ciccotti, H. J. C. Berendsen, *J. Comput. Phys*., 1977, 23, 327.

29 D. A. Case, T. A. Darden, T. E. Cheatham, C. L. Simmerling,J. Wang, R. E. Duke, R. Luo, R. C. Walker, W. Zhang, K. M. Merz, B. Roberts, S. Hayik, A. Roitberg, G. Seabra, J. Swails, A. W. Götz, I. Kolossváry, K. F. Wong, F. Paesani, J. Vanicek, R. M. Wolf, J. Liu, X. Wu, S. R. Brozell, T. Steinbrecher, H. Gohlke, Q. Cai, X. Ye, J. Wang, J. Hsieh, G. Cui, D. R. Roe, D. H. Mathews, M. G. Seetin, R. Salomon-Ferrer, C. Sagui, V. Babin, T. Luchko, S. Gusarov, A. Kovalenko, P. A. Kollman, AMBER 12, University of California, San Francisco ,2012.

30 C. J. Dickson, L. Rosso, R. M, Betz, R. C. Walker, I. R. Gould, *Proteins,* 2012, 8, 9617.

31 J. Wang, R.M. Wolf, J.W. Caldwell, P.A. Kollamn, D.A. Case, J. Comput. Chem., 2004, 25, 1157.

32 http://www.ambermd.org

33 R. Bill, T. D. McGee, J. M. Swails, N. Homeyer, H. Gohlke, A. E. Roitberg, J. Chem. Theory. Comput., 2012, 8, 3314-3321.

34 H. Gohlke, C. Kiel, D. A. Case, *J. Mol. Biol*., 2003, 330, 891.

35 J. Srinivasan, T. E. Cheatham, P. Cieplak, P. A. Kollman, D. A. Case, *J. Am. Chem. Soc*., 1998, 120, 9401.

36 Y. Zhao, D. G. Truhlar, *J. Phys. Chem.*, 2006, 110, 5121.

37 R. J. Bartlett, G. D. Purvis, *Int. J. Quantum Chem*., 1978, 14, 561.

38 M. J. Frisch, G. W. Trucks, H. B. Schlegel, G. E. Scuseria, M. A. Robb, J. R. Cheeseman, J. A. Montgomery, T. Vreven, K. N. Kudin, J. C. Burant, et al. Gaussian 09, revision B.09; Gaussian, Inc.: *Pittsburgh, PA*, 2009.

39 M. Cossi, N. Rega, G. Scalmani, V. Barone, *J. Comput. Chem.,* 2003, 24, 669.

40 Cossi, M.; Barone, V.; Cammi, R.; Tomasi, J., *Chem. Phys. Lett*., 1996, 255, 327.

41 A. E. Reed, L. A. Curtiss, F. Weinhold, *Chem. Rev*., 1988, 88, 899.

42 R. F. W. Bader, Atoms in Molecules, A Quantum Theory; Oxford University Press: New York, 1990.

43 R. F. W. Bader, *Chem. Rev*., 1991, 91, 893.

44 W. Scherer, P. Sirsch, D. Shorokhov, M. Tafipolsky, G. S. McGrady, E. Gullo, *Chem. Eur. J.,* 2003, 9, 6057.

45 A. Shurki, P. C. Hiberty, S. Shaik, *J. Am. Chem. Soc*., 1999, 121, 822.

46 A. D. Becke, K. E. Edgecombe, *J. Chem. Phys.,* 1990, 92, 5397.

47 A. Savin, R. Nesper, S. Wengert, T. Fassler, *Angew. Chem. Int. Ed. Engl.*, 1997, 36, 1808.

48 J. K. Burdett, T. A. McCormick, T. A., *J. Phys. Chem. A,* 1998, 102, 6366.

49 A. Savin, V. Jepsen, J. Flad, O. K. Andersen, H. Preuss, H. G. von Schnering, *Angew. Chem. Int. Ed. Engl*., 1992, 31, 187.

50 V. Tsirelson, A. Stash, *Chem. Phys. Lett*., 2002, 351, 142.

51 H. L. Schmider, A. D. Becke, J. Mol. Struct. Theochem, 2000, 527, 51.

52 H. Jacobsen, *J. Chem.,* 2008, 86, 695.

53 T. Lu, W. Chen, *J. Comput. Chem*., 2012, 33, 580.

54 T. D. Clark, J. M. Buriak, K. Kobayashi, M. P. Isler, D. E. McRee, *J. Am. Chem. Soc.,* 1998, *120*, 8949.

55 J. P. Lewis, N. H. Pawley, O. F. Sankey, *J. Phys. Chem. B,* 1997, 101, 10576.

56 M. Izadyar, M. Gholizadeh, M. Khavani, M. R. Housaindokht, *J. Phys. Chem. A,* 2013, 117, 2427.

57 M. Izadyar, M. Khavani, *Int. J. Quantum Chem*., 2014, 114, 1-9.